 doi:10.20944/preprints202203.0153.v1

Chronic Exposure to Methadone Induces Activated Microglia and Astrocyte and Cell Death in the Cerebellum of Adult Male Rats

Naghmeh Zamani[1], Laya Takbiri Osgoei[2*], Abbas Aliaghaei[3, 4*], Nasim Zamani[5], Hossein Hassanian-Moghaddam[5]

1- Department of Biology, Tehran North Branch, Islamic Azad University, Tehran, Iran.
2- Department of Microbiology, Tehran North Branch, Islamic Azad University, Tehran, Iran.
3- Hearing Disorders Research Center, Loghman-Hakim Hospital, Shahid Beheshti University of Medical Sciences, Tehran, Iran
4- Department of Biology and Anatomical Sciences, School of Medicine, Shahid Beheshti University of Medical Sciences, Tehran, Iran.
5- Department of Clinical Toxicology, Loghman-Hakim Hospital, Shahid Beheshti University of Medical Sciences, Tehran, Iran.

*Corresponding Authors:
Dr. Laya Takbiri Osgoei and **Dr. Abbas Aliaghaei**

 doi:10.20944/preprints202203.0153.v1

Abstract

Background: Methadone is a centrally-acting synthetic opioid analgesic widely used in the methadone maintenance therapy (MMT) programs throughout the world. Considering its neurotoxic effects particularly on the cerebellum, this study aims to address the behavioral and histological alterations in the cerebellar cortex associated with methadone administration.

Materials and Methods: Twenty-four adult male albino rats were randomized into two groups of control and methadone treatment. Methadone was subcutaneously administered (2.5–10 mg/kg) once a day for two consecutive weeks. The functional and structural changes in the cerebellum were compared to the control group.

Results: Our data revealed that treating rats with methadone not only induced cerebellar atrophy, but also prompted the actuation of microgliosis, astrogliosis, and apoptotic biomarkers. We further demonstrated that treating rats with methadone increased complexity of astrocyte processes and decreased complexity of microglia processes. Our result showed that methadone impaired motor coordination and locomotor performance and neuromuscular activity. Additionally, relative gene expression of TNF-α, caspase-3 and RIPK3 increased significantly due to methadone.

Conclusions: Our findings suggest that methadone administration has a neurodegenerative effect on the cerebellar cortex via dysregulation of microgliosis, astrogliosis, apoptosis, and neuro-inflammation.

Keywords: Apoptosis; Cerebellum; Methadone; Neuroinflammation

Preprints (www.preprints.org) | NOT PEER-REVIEWED | Posted: 10 March 2022 doi:10.20944/preprints202203.0153.v1

Introduction

Methadone (6-[dimethylamino]-4,4-diphenyl-3-heptanone) is a synthetic opioid used for the preservation therapy of opiate addicts [1]. Characteristics including high bioavailability of 40–99% [2, 3], long half-life of about 24 hours, and long duration of action ranging between 5 to 130 hours [4] has made it the drug of choice for treatment of drug abuse [5]. However, acute methadone intoxication due to accidental or intentional overdose has been reported to cause neurological mortality and morbidity [6-8]. Its effects on the central nervous system (CNS) have generally been studied in the fetus of rats, raising questions about potential impacts on exposed children during fetal life through their addicted mothers [9].

Rats are appropriate animal models for drug exposure [10-12]. Comparative anatomical research has demonstrated that cerebellum is a protected structure in different species [13] and the presence of opioid cells in the brain of a developing rat is well established [14]. The granule neurons' movement from the external granule layer (EGL) to the internal granule layer (IGL) is completed two weeks after the birth of rats [15]. Migration is driven by many other signals and calcium ion (Ca^{2+}) influx is mediated by the N-methyl-D aspartate receptor (NMDAR) [16]. The cerebellum, due to the prenatal development, is likely to be the target of opioids in the late gestation.

The NMDARs are a subfamily of excitatory ionotropic glutamate receptors considered as cation channels with high permeability ligands for Ca^{2+}. The functional NMDARs consist of four subunits including two NR3 or NR2 and two NR1 subunits [17]. NMDARs play a key role in the development of brain, including excitotoxic neuronal death [18], apoptosis [19], neuronal migration [16], and the neurite outgrowth [20]. The localization and composition of NMDAR subunits are dynamic and change across the CNS, especially in the development process. GluN2B is largely expressed before birth in the rat CNS, while the GluN2A expression begins perinatally. Furthermore, GluN2B is smoothly limited to the forebrain one week after delivery. GluN2B and GluN2A are predominant in higher brain structures in adults, which might indicate that they are related to synaptic plasticity and function [17]. GluN2B expression peaks around PND14 in the rat cerebellum, before GluN2C and GluN2A change into adulthood [21]. Therefore, the expression of various NMDAR subunits, particularly GluN2B, is critical for the plasticity growth of the cerebellum [22].

The short- and long-term complications of methadone have been studied in pregnant rats and its effect on neurodevelopmental dysfunction and growth retardation in the brain of the fetus rats have been reported [22]. Pre-clinical studies suggest that prenatal methadone exposure may alter the development of dopaminergic, cholinergic, and serotonergic systems, and modify myelination. The Antenatal exposure to the drug is associated with behavioral consequences including depression, anxiety, and impaired learning, memory, and social function [23].

Despite some research on the effect of methadone on brain, the precise changes provoked by chronic exposure to methadone in the brain and cerebellum remain unclear. The primary goal of the present study is to clarify the chronic consequences of methadone on cerebellar cells in rats.

Preprints (www.preprints.org) | NOT PEER-REVIEWED | Posted: 10 March 2022 doi:10.20944/preprints202203.0153.v1

MATERIALS AND METHODS

Reagents

Methadone hydrochloride 5 mg/ml was purchased from Darou-Pakhsh Pharmaceutical Company, Tehran, Iran. Antibodies against Iba-1(ab5076), GFAP (ab7260), caspase-3 (ab32351), goat anti rabbit IgG conjugated TRITC (ab6718), and Mouse and Rabbit Specific HRP/DAB (ABC). Detection immunohistochemical (IHC) kits (ab64264) were purchased from ABCAM (ABCAM Co., Cambridge, UK). Other material was procured from Sigma Aldrich (St. Louis, Mo, USA).

Animals and treatment protocols

Twenty-four adult male albino rats weighing 200–220 g were taken from the animal lab at Shahid Beheshti University of Medical Sciences. The research was approved by the Animal Care and Use Committee of Shahid Beheshti University of Medical Sciences (IR SBMU.MSP.REC.1398.292). Rats were nurtured and kept at the animal room with controlled 12-h light/dark cycles and a temperature of 18 to 22^{o}C. They were randomized into two groups of control and methadone treatment (n=12 in each group). In the methadone group, methadone was dissolved in 0.9% saline and stored at room temperature. The rats were injected with this solution once a day for two weeks with increasing doses. The injection dose was 2.5 mg/kg in the two first days and 5 mg/kg in the following three days during the first week. In the second week, the dose was increased to 10 mg/kg. The control group was injected with 0.9% saline. All injections were performed subcutaneously (SC) in a dose of 1 ml/kg at 8–10 AM. They were administered biweekly alternating between right and left side of the lower back. The maximum dose (10 mg/kg) was chosen based on LD50 for methadone in rats, which is 30 mg/kg and 9 mg/kg for oral and intravenous (IV) administration, respectively (www.bionichepharmausa.com)[24].

Evaluation of the motor coordination in treated rats

The rotarod performance test was run after 1 and 2 weeks. Rats were placed on an accelerating cylinder with a velocity of 4 to 40 rpm in 300-second test sessions. If rats fell from the rung or grasped it and spun for two consecutive revolutions without any effort to run, they were excluded (a total of 2). Finally, the maximum time spent by each rat in the task was recorded.

Locomotor Activity Measurement

Animal behavior was studied using the open-field test. The test was conducted during the final administration of methadone by placing animals into a 90× 90-cm area. The total distance travelled was recorded automatically by a monitoring system. At the end of each experiment session, animals were returned to their cages. The area was cleaned, dried, and prepared for the next trial. Moreover, to prevent any environmental disturbance, all behavioral tests were performed in a close and quiet room. At the beginning of the experiment, each rat was placed at the corner of the device floor with the ability to move and explore the apparatus for five minutes. In addition to the distance travelled and the time spent at the center, periphery and corners of the apparatus were quantified utilizing Ethovision® XT video tracking software (Noldus) mounted with a digital video camera.

Electromyography (EMG) Recording

Preprints (www.preprints.org) | NOT PEER-REVIEWED | Posted: 10 March 2022 doi:10.20944/preprints202203.0153.v1

The EMG recording was performed after the open field testing. Initially, the rats were deeply anesthetized by intraperitoneal injection of a cocktail of ketamine hydrochloride (60 mg/kg) and xylazine (8 mg/kg) using insulin syringes. The intervention site on the right hind limb of the rats was then disinfected by the povidone-iodine solution. The skin of the posterior thigh of each animal was incised 3 cm longitudinally from the greater trochanter to the popliteal fossa. To expose the sciatic nerve, the gluteus maximus and biceps femoris muscles were dissected along with the gastrocnemius muscle. To record electrical oscillation, two monopolar subdermal teflon needle electrodes were arranged in parallel at a fixed distance of 7 mm from each other. Ringer's solution was also used to hinder neural death during the procedure. Finally, the sciatic nerve was stimulated (1 A, 0.2-Hz frequency, for 100 s) and the action potentials of gastrocnemius muscle ipsilateral to the site of intervention were recorded. The desired parameter was the latency of the compound muscle action potential.

Immunohistochemistry

During the first step of IHC process, rats were deeply anesthetized by 100 mg/kg ketamine and 10 mg/kg xylazine; rats were then transcardially perfused with chilled saline and fixed by a fixator containing 4% paraformaldehyde in 0.1 M phosphate-buffered saline (PBS). Cerebellums were then extracted and placed in formalin before being prepared and placed on the slides. Formalin-fixed tissues were embedded in paraffin wax. Paraffin-embedded tissue section is normally sliced by a rotary microtome (Thermo Fisher Scientific, Waltham, MA, USA) to give a thickness of 6 µm. The slide is immersed in xylene to remove the paraffin and transferred through a series of diluted alcohols (100%, 95%, 70%, and 50%) to water prior to staining. Afterwards, antigen retrieval was carried out before immunohistochemistry (0.01 M citrate buffer solution (pH 6.0), 0.01 M PBS buffer (pH7.0), 0.05 M EDTA (pH 8.0), 0.05 M Tris-EDTA (pH 9.0), 0.05 M Tris-HCl). The primary antibodies were anti-Iba-1 antibody (1: 300), GFAP antibody (1: 100) and anti-caspase-3 (1: 300) diluted in the PBS solution containing 0.3% Triton X-100 and 1% bovine serum albumin (BSA). Sections were incubated in the primary antibodies overnight at 4 °C. Consequently, they were incubated with secondary antibodies of avidin-biotin complex substrate in 0.05 m Tris-buffer (pH 7.6) containing 0.05 % 3, 3-diaminobenzidine tetrahydrochloride, and 0.03% hydrogen peroxide or secondary fluorescent TRITC-conjugated antibody (1:500). After immunohistochemical reaction, sections were mounted by Mounting Medium for IHC (Abcam. Cambridge, UK, ab64230), counter-stained, and observed under a microscope.

Sholl Analysis for Iba-1 Labeled Microglia and GFAP Labeled Astrocyte

Sholl analysis was performed on Iba-1 and GFAP immunostaining using the ImageJ software (Java. NIH, USA). The microscopic images required for the analysis were captured by a 40X objective lens (Nikon Eclipse E-100). As described in a previous study [25], a total of thirty individual microglia and astrocyte were selected for the reconstruction. For the direct analysis, each figure was imported to ImageJ after setting the image scale and marking the nucleus at the center. To determine the nearest neighbor distance (NND), a script for Fiji (ImageJ) developed by Y.Mao [26] was used as explained in a previous study [27]. After analysis, the results for each cell were saved in a separate file.

RNA extraction

Preprints (www.preprints.org) | NOT PEER-REVIEWED | Posted: 10 March 2022 doi:10.20944/preprints202203.0153.v1

Based on the instructions of the manufacturers of Trizol and RNeasy Lipid Tissue Mini Kit (Qiagen, USA), hippocampus lysates of six rats from each group were pooled for total RNA isolation. Saline and a tramadol sample were prepared from the RNAs extracted from the pooled hippocampus lysates. Samples were washed in 25 µL of RNase-free H2O, quantified by a Nanodrop ND-1000 (Thermo Fisher Scientific) spectrophotometer and RNA qualities were assessed by applying Agarose Gel Electrophoresis and Bioanalyzer 2100 (Agilent Technologies Inc. CA, USA). All samples showed a concentration of >100 ng/µl and an RNA integrity number (RIN) of ≥8.

Quantitative real-time PCR

Quantitative real-time PCR (qPCR) was carried out using specific primers for TNFα, IL-1β, caspase-3, RIPK3 and GAPDH were used as the reference genes (Table 1).

Data analysis

All statistical analyses were carried out using SPSS software version 23 (IBM Incorporations, Chicago, Ill, USA). The graphs were created by Graph Pad Prism 7. Data was presented as mean ± SEM. Differences between experimental groups was evaluated using the independent sample t-test. P values lower than 0.05 were considered as significant.

Preprints (www.preprints.org) | NOT PEER-REVIEWED | Posted: 10 March 2022 doi:10.20944/preprints202203.0153.v1

Results

Methadone significantly decreased spontaneous locomotor activity, anxiety-like behavior, and neuromuscular activity

To evaluate whether methadine impacts motor coordination, the rotarod test was performed. Motor coordination was significantly impaired in the methadone-treated group as opposed to the control group and the methadone-treated rats were inferior to the control at 1st ($P<0.001$) and 2nd ($P<0.001$) weeks (Fig. 1a). Administration of methadone had a significant effect on locomotor activity in rats. As illustrated in Fig. 1b, the spontaneous locomotor activity declined in rats treated with methadone compared to the control group ($P<0.001$). Also, the analysis of open field data showed that the duration of rats' immobility in the center of the field (as an indicator of anxiety) dropped significantly in the methadone group compared to the control group ($P<0.001$) (Fig. 1c). Moreover, the neuromuscular activity of the methadone-treated rats decreased significantly due to the increased EMG latency as opposed to the control group ($P<0.05$) (Fig. 2).

Methadone administration upregulated Caspase-3 expression

After the administration of methadone for 2 weeks, immunohistochemistry was performed on cerebellum samples to determine Caspase-3 expression. Caspase-3 immunoreactivity was approximately 2.5-fold higher in the rats treated with methadone compare to the control group ($P <0.001$) (Fig. 3).

Methadone significantly increased microgliosis marker Iba-1 in rats' cerebellum

Iba1-specific antibody was utilized to demonstrate microgliosis and morphological features of microglial cells (Fig. 4a). The immunohistochemistry findings in the present study revealed a surge in the number of Iba-1 positive cells in the cerebellum of the rats treated with methadone compared to the control group ($P<0.05$) (Fig. 4b). To examine the morphology of the microglia, Iba-1 positive cells were submitted to the Sholl analysis. The results showed a significant drop in the NND in the methadone group as opposed to the control group ($P<0.001$) (Fig. 4c).

Chronic administration of methadone increased microglia activation

For the analysis of the microglia morphology, Iba-1 positive cells were submitted to the Sholl analysis. The results revealed that the complexity of microglia processes decreased in methadone significantly ($P<0.05$) (Fig.5a). Our results indicate that methadone could significantly increase the soma size of microglia ($P<0.05$) (Fig. 5b). On the other hand, the total length of microglia process dwindled in the methadone group in comparison to the control group ($P<0.01$) (Fig. 5c).

Preprints (www.preprints.org) | NOT PEER-REVIEWED | Posted: 10 March 2022 doi:10.20944/preprints202203.0153.v1

Chronic administration of methadone reduces astrogliosis and alters astrocyte morphology

The findings suggested that methadone treatment increased the number of GFAP-positive cells in the methadone-receiving group as opposed to the control group ($P<0.001$) (Fig. 6a, b). To study the morphology of astrocytes, Sholl analysis was conducted on GFAP-positive cells. The results exhibited a significant decrease in the NND in the methadone group as opposed to the control group ($P<0.001$) (Fig. 6c). Our results showed that the complexity of astrocyte processes increased in methadone group ($P<0.05$) (Fig.7a) Moreover, a substantial increase in soma size was observed in the methadone group versus the control group ($P<0.001$) (Fig. 7b). Additionally, total astrocyte process length increased in methadone group compared to the controls, but this increase was not statistically significant (Fig. 7c).

Methadone induced differential gene expression of inflammation, apoptosis, and necroptosis in the cerebellum

The expression levels of inflammation-associated genes were examined by real-time qPCR (Fig. 8). The pro-inflammatory cytokines (*TNF-α*) increased substantially upon methadone treatment ($P<0.01$) but expression of *IL1β* was not statistically significant. Moreover, the expression levels of *caspase-3* were also measured in the cerebellum (Fig. 8). According to our results, methadone led to a remarkable increase in the expression of *caspase-3* in the cerebellum ($P<0.05$). According to qPCR results, the relative expression of the intrinsic necroptosis related gene (*RIPK3*) was drastically higher in methadone-treated groups than in the control ($P<0.05$) (Fig. 8).

Preprints (www.preprints.org) | NOT PEER-REVIEWED | Posted: 10 March 2022 doi:10.20944/preprints202203.0153.v1

DISCUSSION

The impact of opioid exposure on the brain of humans, animals, newborns, and children has been the subject of many studies. In animals, it has been shown that opioids like methadone and buprenorphine can have adverse effects on the CNS. On the other hand, certain alterations in myelination and oligodendrocyte maturation are induced following changes in myelin thickness, axon size, cholinergic neuron production, and decreased nerve expression of growth factor in the striatum [28-30]. Additionally, morphine exposure in utero decreases the size and number of Purkinje cell numbers in the cerebellum of the neonatal mice [31]. Pregnant mice's pups exposed to heroin displayed altered apoptosis protein exposure in the hippocampus, which is vital for memory and learning [32]. Morphine can also enhance the rate of apoptosis in neuronal cells and microglia in the human fetus [33, 34]. Different areas of brain have been shown to be affected by methadone [35]. Several studies have reported that narcotics can alter the locomotor activity [36]. The results of studies with extensive doses generally suggest that narcotics can both elevate and reduce the activity depending on the dose and elapsed time since injection [37]. Previous research suggests that certain effects of morphine are mediated by the release of catecholamines from adrenergic neurons in the brain.

Our motor activity analysis showed diminished motor function of rats in the methadone group. We also observed mounting anxiety in this group of rats. Methadone can function both as an antagonist for *the N*-methyl-*d*-aspartate receptor (NMDA), and an agonist for the mu-opioid receptor [38]. Mu-opioid receptors, which mainly reside in the limbic system and the cerebellum can enhance the impacts of opioids by simplifying the long-term potentiation [39]. The globous pallidus, basal ganglia, and hippocampus have been shown to be prone to hypoxia caused by short-term memory deficits and alterations in physical and cognitive functions [40, 41]. However, some previous studies have reported impaired executive function and motor coordination after methadone overdose [42, 43]. The administration of NMDA receptor antagonists such as MK-801 and AP5 can tamper with the spatial working memory. Thus, methadone antagonistic actions on the NMDA receptors may support the hypothesis that methadone regulates via both NMDA and opioid receptors to exert neurotoxic/adverse impacts on motor function and memory in several behavioral actions [12, 44-46].

Our EMG analysis suggested impaired nerve function of the muscle in the methadone group. Various neuromodulation and neurotransmitter systems seem to undergo changes in the cerebellum of animals acutely exposed to opioids, along with alterations in the intracellular signaling molecules. Cholinergic transmission is associated with various abused drug actions [47-49]. Cholinergic receptors have been demonstrated to exist in different layers of the cerebellum [50, 51], and alterations in this system can modify the behavior of synaptic plasticity and cerebellar neurons [52-54]. According to this system, morphine injection could increase cerebellar acetylcholine concentrations [55], but might reduce the total level of choline acetyltransferase [56]. There is a growing body of research on high methadone-induced leukoencephalopathy, which may be detected by the magnetic resonance imaging [57, 58]. The underlying mechanism is still unclear, but it is hypothesized to be partly due to the lack of energy metabolism, which is caused by demyelination after respiratory arrest/depression following methadone overdose [59]. The direct activation or damaged immunological reactions to the brain tissue is another possible hypothesis that explains pathogenesis involvement in the methadone-induced leukoencephalopathy [57, 58, 60, 61]. It has been reported that methadone toxicity in the cell culture

provokes methadone-induced cell death that cleaves mitochondria and leads to the impaired ATP synthesis [62].

The results also indicate that methadone administration can cause cell death in the cerebellum, which is associated with the augmented expression of caspase-3 protein. Recent investigations show that caspase proteases are crucially involved in the signal transduction route and contribute to the apoptosis [63, 64]. It has been declared that apoptotic properties induced by loperamide and buprenorphine were determined by Z-Asp-CH2-DCB, a caspase inhibitor with a wide range of selectivity [65, 66] following assessment by DNA-laddering analysis and flow cytometry. These outcomes imply that the caspase inhibitors can block the apoptosis induced by some anticancer treatments such as camptothecine, etoposide, and adriamycin [67]. YOSHIDA et al. reported that treatment with buprenorphine could generate an active caspase-3-like protease through the conversion process, generating apoptotic properties like nuclear fragmentation and DNA laddering. Lately, it has been reported that caspase-3 triggers the caspase-3-activated DNase (CAD), leading to DNA fragmentation via the digestion process of an CAD inhibitor [68, 69].

The immunohistochemical results suggest that methadone increases microgliosis. Microglia are inflammatory cells in the brain, and their increased number may be associated with inflammation. The link between the function/expression of mu opioid receptor (MOR) and microglial activation has been further studied, particularly by *in vitro* investigations on the primary murine microglial cultures. Low levels of DAMGO, as a selective agonist of MOR, along with morphine triggered the rat microglia, but this activation process was later prevented by the MOR-selective antagonist D-Phe-Cys-Tyr-D-Trp-ArgThr-Pen-Thr-NH2 (CTAP) [70]. The expression of Toll-like receptors (TLRs) is enhanced by morphine and weakened by the MOR-selective antagonist D-Phe-Cys-Tyr-D-Trp-Orn-Thr-Pen-ThrNH2 (CTOP). In addition, this effect of morphine was reversed in the mouse microglia cultured with the MOR knockout (KO) [71]. Morphine activated the PKCe-Akt-ERK1/2 kinase route and enhanced the cytokine expression in the murine microglia, but these impacts could be prevented by *Oprm1* RNA silencing and by CTAP [72, 73]. Low concentration of morphine has been shown to improve NF-kB function through MOR, which is inhibited by CTAP. On the other hand, a high level of morphine induced non-opioid response mediated by the TLR4 [74, 75].

In the present study, the IHC analysis manifested a surge in the number of astrogliosis in the methadone group. The growing number of astrocytes is a pathologic event that reflects damages to the neural tissue. Moreover, the relationship between astrocytes and microglia can cause inflammation. The simultaneous activation of microglia and astrocytes has also been shown during chronic morphine administration. In particular, chronic injections of morphine in rats trigger both spinal astrocytes and microglia with the release of TNF-a [76]. In animals with neuropathic conditions, both microglia and spinal astrocytes could be activated by the chronic intake of morphine. In addition, morphine analgesia and glial activation are mitigated following a chronic concomitant therapy with botulinum toxin, which suggests a potential clinical use [77]. The simultaneous activation of astrocytes and microglia has also been reported in the ventrolateral periaqueductal gray matter (vlPAG) after several injections of morphine, suggesting that glial cells and neurons are involved in opioid-induced hyperalgesia (OIH)-related process in the PAG [78]. Furthermore, consistent peripheral inflammation reduced the chronic morphine activation of microglia and astrocytes in vlPAG and swindled analgesic tolerance, exhibiting a long-distance peripheral damage to the PAG-mediated OIH processes [79]. Subsequently, similar outcomes were observed in the pattern that peripheral inflammation affected analgesic tolerance [80]. Lin et al. presented a new approach for quantifying various parameters of astrocyte and microglia activation in OIH, which can

Preprints (www.preprints.org) | NOT PEER-REVIEWED | Posted: 10 March 2022 doi:10.20944/preprints202203.0153.v1

improve glia activation mechanisms in OIH in the future [81]. Furthermore, while morphine activates astrocytes-microglia and OIH, several new endomorphine derivatives provide less tolerance following a deficit in glia activation or OIH [82]. This suggests that mu opioid agonists with analgesic features but without adverse effects following glia could be improved [83]. These can explain our findings. Several studies on the transcription of microglia have reported the concurrent regulation of gene modules or subsets, which allow place microglia in the class of subspecies that express high concentrations of special gene modules [75].

For the first time, the results of Sholl analysis in our study showed astrocytes hypertrophy in the methadone group suggesting reactive astrocytes. It means that astrocytes, aggressive in this state, can inflict damage on the neural tissue. The term reactive astrogliosis, also known as the reactive gliosis, explains astrocytes' reactions in conditions like stroke, spinal cord or brain trauma, neurodegenerative disorders, or epilepsy. This reaction has been described as a multi-stage, graded, conserved, and constitutive defensive astroglia response [84]. Compared to astrocytes in the CNS with no damages, reactive astrocytes alter their function and morphology, which is demonstrated by the altered expression of several genes [85-89]. Reactive astrocytes exhibit some morphological and molecular properties, the most prominent feature of which is the upregulation of the glial fibrillary acidic protein. Also, a major part of the astrocyte intermediate filament structure is considered the nanofilament structure. The upregulation of GFAP and some other symptoms of astrocyte reactivity is related to a range of neuropathologies, such as diabetic retinopathy, stroke, neuroinflammation, brain hemorrhage, Batten disease, CNS tumors, epilepsy, amyotrophic lateral sclerosis, retinal ischemia, Parkinson's disease, neurotrauma, Alzheimer's disease, or multiple sclerosis. Some cytokines such as leukemia inhibitory factor (LIF), oncostatin M, interleukin-6, and transforming growth factor-α, or ciliary neurotrophic factor have been shown to activate astrocytes [90-95]. The astrocytes can be activated by the gp-130/ activator of transcription 3 (STAT3) signaling route, or latter nuclear translocation and phosphorylation of STAT3 in the astrocytes [94, 96].

The results of the present study also suggest that methadone can induce M1 or toxic phase microglia. Factors associated with the expression of opioids in glial and immune cells can explain inconsistencies in the findings about the composition of cell population (such as microglia or astrocytes, lymphocytes, monocytes, macrophages, granulocytes), their subgroups (including M2 or M1 macrophages, B or T lymphocytes, microglia, or T helper 2 or T helper 1 lymphocytes), their original tissue, duration and type of the pathological state, physiological vs. pathological conditions and *in vivo* or *in vivo* pharmacological drugs [97]. Based on the M1 phenotype, microglia generate neurotoxic molecules and pro-inflammatory cytokines, which trigger cytotoxic and inflammation reactions. In contrast, M2 phenotypes release nutrient factors and anti-inflammatory cytokines which enhance the function of regeneration, restore, and repair homeostasis [98].

In this study, the expression levels of inflammatory genes, as well as apoptosis and necroptosis, were higher in the methadone group than in the control group, according to real-time analysis. During disease or injury, astrocytes can detect endogenous "danger signals," which are generated by injured cells to alarm the immune system [99]. The recognition of these molecules is possible by the expression of astrocytic of specific pattern-recognition receptors, such as different members of the Toll-like receptor family [100]. TLR3 is expressed strongly in astrocytic cells in brain tissues and *in vitro* [101-103], however TLR2, TLR9, TLR5, TLR4, and are only found at low levels in astrocyte cultures [101, 102]. *In*

Preprints (www.preprints.org) | NOT PEER-REVIEWED | Posted: 10 March 2022 doi:10.20944/preprints202203.0153.v1

vitro stimulation of astrocytic TLRs, on the other hand, appears to trigger a positive feedback loop that leads to increased expression of several of these receptors, including TLR2, TLR4, and TLR3 [104, 105]. TLR activation can also trigger fast immunological responses in astrocytes, resulting in the production and secretion of a variety of mediators, including chemokines and cytokines [101, 103-105]. The ability of microglia and astrocytes is to produce the cytokines IL-1, IL-10, IL-6, interferon g (IFN-g), TNF-α, Granulocyte- TGF-β, and Macrophage Colony-Stimulating Factor (GM-CSF), as well as the chemokines CCL20, (C–C motif) ligand (CCL) 2, (C–X–C motif) ligand, and CCL5 [100]. Some of these mediators have been found to have the ability to activate nearby glial cells as well as draw immune cells from the bloodstream, thereby increasing local immunological responses in the CNS [100]. These elements appear to be aimed at the astrocytes themselves. In fact, genetic manipulation or intracerebral injections of IFN-γ, IL-2, IL-1, TNF-α, IL-6, or TGF-β revealed that these cytokines have a role in inducing extensive astrocytosis *in vivo* [90, 106-108].

Excessive production of toxic chemicals (e.g., free radicals, NO) or cytokines can result in astrocytic malfunction and cell death [109-111], which can worsen neurodegeneration and neuronal dysfunction [109-111]. Several lines of evidence suggest that TLR-4 and IL-1RI stimulation can activate NF-κB pathways and MAP kinases, potentially leading to the generation of inflammatory mediators such as TNF-α, COX-2, iNOS, IL-1, and IL-12, [112]. MAPK signaling cascades, which include the protein kinases ERK1/2, P38, and JNK, are critical for the start of cellular processes such as inflammatory responses, apoptosis, proliferation, and stress [110, 113-115].

This study explored the precise effect of methadone on the cerebellum, which can be of great significance in developing new therapeutic strategies for the opioid use or assessment of neuronal markers related to the vulnerability. This, in turn, can reduce the enormous costs that opioid-related diseases impose on the society.

 doi:10.20944/preprints202203.0153.v1

Acknowledgements
We are thankful for the funding provided by Hearing Disorders Research Center, Loghman Hakim Hospital, Shahid Beheshti University of Medical Sciences, and Tehran, Iran.

Conflict of interest

The authors declare no conflict of interest.

Authors' contributions
AA and LTO designed and conceived the study, analyzed and interpreted the data; NZ performed the experiments; NZ wrote the manuscript; HHM had a crucial role in data collection, revised the manuscript and drafted the manuscript for the intellectual content.

 doi:10.20944/preprints202203.0153.v1

References

1. Corkery, J.M., et al., *The effects of methadone and its role in fatalities.* Human Psychopharmacology: Clinical and Experimental, 2004. **19**(8): p. 565-576.
2. Foster, D.J., et al., *Steady-state pharmacokinetics of (R)-and (S)-methadone in methadone maintenance patients.* British journal of clinical pharmacology, 2000. **50**(5): p. 427-440.
3. Foster, D.J., et al., *Population pharmacokinetics of (R)-,(S)-and rac-methadone in methadone maintenance patients.* British journal of clinical pharmacology, 2004. **57**(6): p. 742-755.
4. Eap, C.B., T. Buclin, and P. Baumann, *Interindividual variability of the clinical pharmacokinetics of methadone.* Clinical pharmacokinetics, 2002. **41**(14): p. 1153-1193.
5. Farid, W., et al., *The effects of maternally administered methadone, buprenorphine and naltrexone on offspring: review of human and animal data.* Current neuropharmacology, 2008. **6**(2): p. 125-150.
6. Shields, L.B., et al., *Methadone toxicity fatalities: a review of medical examiner cases in a large metropolitan area.* Journal of Forensic Sciences, 2007. **52**(6): p. 1389-1395.
7. Stinson, F.S., et al., *Comorbidity between DSM-IV alcohol and specific drug use disorders in the United States: results from the National Epidemiologic Survey on Alcohol and Related Conditions.* Drug and alcohol dependence, 2005. **80**(1): p. 105-116.
8. Ahmad-Molaei, L., et al., *Time-Dependent Changes in the Serum Levels of Neurobiochemical Factors After Acute Methadone Overdose in Adolescent Male Rat.* Cellular and Molecular Neurobiology, 2020: p. 1-15.
9. Zagon, I.S. and P.J. McLaughlin, *Comparative effects of postnatal undernutrition and methadone exposure on protein and nucleic acid contents of the brain and cerebellum in rats.* Developmental neuroscience, 1982. **5**(5-6): p. 385-393.
10. Newby-Schmidt, M. and S. Norton, *Development of opiate tolerance in the chick embyro.* Pharmacology Biochemistry and Behavior, 1981. **15**(5): p. 773-778.
11. Sun, H., et al., *Detour behavior changes associated with prenatal morphine exposure in 11-day-old chicks.* International Journal of Developmental Neuroscience, 2010. **28**(3): p. 239-243.
12. Ebert, B., S. Andersen, and P. Krogsgaard-Larsen, *Ketobemidone, methadone and pethidine are non-competitive N-methyl-D-aspartate (NMDA) antagonists in the rat cortex and spinal cord.* Neuroscience letters, 1995. **187**(3): p. 165-168.
13. Sultan, F. and M. Glickstein, *The cerebellum: comparative and animal studies.* The cerebellum, 2007. **6**(3): p. 168-176.
14. Vernadakis, A., et al., *Function of opioids early in embryogenesis.* Annals of the New York Academy of Sciences, 1990. **579**(1): p. 109-122.
15. Hager, G., et al., *Novel forms of neuronal migration in the rat cerebellum.* Journal of neuroscience research, 1995. **40**(2): p. 207-219.
16. Komuro, H. and P. Rakic, *Modulation of neuronal migration by NMDA receptors.* Science, 1993. **260**(5104): p. 95-97.
17. Paoletti, P. and P. Ascher, *Mechanosensitivity of NMDA receptors in cultured mouse central neurons.* Neuron, 1994. **13**(3): p. 645-655.
18. Ikonomidou, C., et al., *Blockade of NMDA receptors and apoptotic neurodegeneration in the developing brain.* Science, 1999. **283**(5398): p. 70-74.
19. Gupta, K., G.E. Hardingham, and S. Chandran, *NMDA receptor-dependent glutamate excitotoxicity in human embryonic stem cell-derived neurons.* Neuroscience letters, 2013. **543**: p. 95-100.

20. Pearce, I.A., M.A. Cambray-Deakin, and R.D. Burgoyne, *Glutamate acting on NMDA receptors stimulates neurite outgrowth from cerebellar granule cells.* Febs Letters, 1987. **223**(1): p. 143-147.
21. Monyer, H., et al., *Developmental and regional expression in the rat brain and functional properties of four NMDA receptors.* Neuron, 1994. **12**(3): p. 529-540.
22. Fjelldal, M.F., et al., *Opioid receptor-mediated changes in the NMDA receptor in developing rat and chicken.* International Journal of Developmental Neuroscience, 2019. **78**: p. 19-27.
23. Monnelly, V.J., et al., *Prenatal methadone exposure is associated with altered neonatal brain development.* NeuroImage: Clinical, 2018. **18**: p. 9-14.
24. Andersen, J.M., et al., *Long-term methadone treatment impairs novelty preference in rats both when present and absent in brain tissue.* Pharmacology Biochemistry and Behavior, 2011. **98**(3): p. 412-416.
25. Moghaddam, M.H., et al., *Elderberry diet ameliorates motor function and prevents oxidative stress-induced cell death in rat models of Huntington disease.* Brain Research, 2021. **1762**: p. 147444.
26. Mao, Y., *Nearest neighbor distances calculation with ImageJ*. 2016.
27. Davis, B.M., et al., *Characterizing microglia activation: a spatial statistics approach to maximize information extraction.* Scientific reports, 2017. **7**(1): p. 1-12.
28. Sanchez, E.S., et al., *Opioid addiction and pregnancy: perinatal exposure to buprenorphine affects myelination in the developing brain.* Glia, 2008. **56**(9): p. 1017-1027.
29. Robinson, S.E., *Effects of perinatal buprenorphine and methadone exposures on striatal cholinergic ontogeny.* Neurotoxicology and teratology, 2002. **24**(2): p. 137-142.
30. Wu, V.W., et al., *Perinatal opioids reduce striatal nerve growth factor content in rat striatum.* European journal of pharmacology, 2001. **414**(2-3): p. 211-214.
31. Golalipour, M.J. and S. Ghafari, *Purkinje cells loss in off spring due to maternal morphine sulfate exposure: a morphometric study.* Anatomy & cell biology, 2012. **45**(2): p. 121-127.
32. Wang, Y. and T.-Z. Han, *Prenatal exposure to heroin in mice elicits memory deficits that can be attributed to neuronal apoptosis.* Neuroscience, 2009. **160**(2): p. 330-338.
33. Hu, S., et al., *Morphine induces apoptosis of human microglia and neurons.* Neuropharmacology, 2002. **42**(6): p. 829-836.
34. Caritis, S.N. and A. Panigrahy, *Opioids affect the fetal brain: reframing the detoxification debate.* American journal of obstetrics and gynecology, 2019. **221**(6): p. 602-608.
35. Berridge, K.C., *The debate over dopamine's role in reward: the case for incentive salience.* Psychopharmacology, 2007. **191**(3): p. 391-431.
36. Middaugh, L.D., D.K. Ingram, and M.A. Reynolds, *Methadone effects on locomotor activity of young and aged mice.* Neurobiology of aging, 1983. **4**(2): p. 157-161.
37. Plonsky, M. and P.R. Freeman, *The effects of methadone on the social behavior and activity of the rat.* Pharmacology Biochemistry and Behavior, 1982. **16**(4): p. 569-571.
38. Doi, S., et al., *Characterization of methadone as a β-arrestin-biased μ-opioid receptor agonist.* Molecular Pain, 2016. **12**: p. 1744806916654146.
39. Klenowski, P., M. Morgan, and S.E. Bartlett, *The role of δ-opioid receptors in learning and memory underlying the development of addiction.* British journal of pharmacology, 2015. **172**(2): p. 297-310.
40. Barash, J.A., N. Somerville, and A. DeMaria Jr, *Cluster of an unusual amnestic syndrome—Massachusetts, 2012–2016.* MMWR. Morbidity and mortality weekly report, 2017. **66**(3): p. 76.
41. Betts, A.M., J.L. Ritter, and W.S. Kubal, *Reversible delayed posthypoxic leukoencephalopathy after drug overdose: MRI findings in a collection of patients.* Emergency radiology, 2012. **19**(2): p. 165-173.

42. Hauser, K. and J. Matthes, *Medical students' medication communication skills regarding drug prescription—a qualitative analysis of simulated physician-patient consultations.* European journal of clinical pharmacology, 2017. **73**(4): p. 429-435.
43. Ocek, T., et al., *Psychodermatology: knowledge, awareness, practicing patterns, and attitudes of dermatologists in Turkey.* The primary care companion for CNS disorders, 2015. **17**(2).
44. Crone, J.S., et al., *Impaired consciousness is linked to changes in effective connectivity of the posterior cingulate cortex within the default mode network.* Neuroimage, 2015. **110**: p. 101-109.
45. Tsien, J., *Huerta PT, and Tonegawa S.* The essential role of hippocampal CA1 NMDA receptor-dependent synaptic plasticity in spatial memory. Cell, 1996. **87**: p. 1327-1338.
46. Ahmad-Molaei, L., et al., *Delay-dependent impairments in memory and motor functions after acute methadone overdose in rats.* Frontiers in pharmacology, 2018. **9**: p. 1023.
47. Williams, M.J. and B. Adinoff, *The role of acetylcholine in cocaine addiction.* Neuropsychopharmacology, 2008. **33**(8): p. 1779-1797.
48. Steidl, S., et al., *Opioid-induced rewards, locomotion, and dopamine activation: A proposed model for control by mesopontine and rostromedial tegmental neurons.* Neuroscience & Biobehavioral Reviews, 2017. **83**: p. 72-82.
49. Mark, G.P., et al., *Cholinergic modulation of mesolimbic dopamine function and reward.* Physiology & behavior, 2011. **104**(1): p. 76-81.
50. Neustadt, A., A. Frostholm, and A. Rotter, *On the cellular localization of cerebellar muscarinic receptors: an autoradiographic analysis of weaver, reeler, Purkinje cell degeneration and staggerer mice.* Brain research bulletin, 1988. **20**(2): p. 163-172.
51. Graham, A., et al., *Immunohistochemical localisation of nicotinic acetylcholine receptor subunits in human cerebellum.* Neuroscience, 2002. **113**(3): p. 493-507.
52. Crepel, F. and S. Dhanjal, *Cholinergic mechanisms and neurotransmission in the cerebellum of the rat. An in vitro study.* Brain research, 1982. **244**(1): p. 59-68.
53. Takayasu, Y., et al., *Muscarine-induced increase in frequency of spontaneous EPSCs in Purkinje cells in the vestibulo-cerebellum of the rat.* Journal of Neuroscience, 2003. **23**(15): p. 6200-6208.
54. Rinaldo, L. and C. Hansel, *Muscarinic acetylcholine receptor activation blocks long-term potentiation at cerebellar parallel fiber–Purkinje cell synapses via cannabinoid signaling.* Proceedings of the National Academy of Sciences, 2013. **110**(27): p. 11181-11186.
55. Romano, J. and T.-M. Shih, *Cholinergic mechanisms of analgesia produced by physostigmine, morphine and cold water swimming.* Neuropharmacology, 1983. **22**(7): p. 827-833.
56. Moreno-Rius, J., *Opioid addiction and the cerebellum.* Neuroscience & Biobehavioral Reviews, 2019. **107**: p. 238-251.
57. Cerase, A., et al., *Methadone-Induced Toxic Leukoencephalopathy: Diagnosis and Follow-up by Magnetic Resonance Imaging Including Diffusion-Weighted Imaging and Apparent Diffusion Coefficient Maps.* Journal of Neuroimaging, 2011. **21**(3): p. 283-286.
58. Mittal, M., et al., *Methadone-induced delayed posthypoxic encephalopathy: clinical, radiological, and pathological findings.* Case reports in medicine, 2010. **2010**.
59. Weinberger, L., et al., *Delayed postanoxic demyelination and arylsulfatase-A pseudodeficiency.* Neurology, 1994. **44**(1): p. 152-152.
60. Mills, F., et al., *Severe cerebellitis following methadone poisoning.* Pediatric radiology, 2008. **38**(2): p. 227-229.
61. Rando, J., et al., *Methadone overdose causing acute cerebellitis and multi-organ damage.* The American journal of emergency medicine, 2016. **34**(2): p. 343. e1-343. e3.
62. Perez-Alvarez, S., et al., *Methadone induces necrotic-like cell death in SH-SY5Y cells by an impairment of mitochondrial ATP synthesis.* Biochimica et Biophysica Acta (BBA)-Molecular Basis of Disease, 2010. **1802**(11): p. 1036-1047.

63. Wang, L., et al., *Ich-1, an Ice/ced-3-related gene, encodes both positive and negative regulators of programmed cell death.* Cell, 1994. **78**(5): p. 739-750.
64. Nicholson, D.W., et al., *Identification and inhibition of the ICE/CED-3 protease necessary for mammalian apoptosis.* Nature, 1995. **376**(6535): p. 37-43.
65. Yokoyama, Y., et al., *CPP32 activation during dolichyl phosphate-induced apoptosis in U937 leukemia cells.* FEBS letters, 1997. **412**(1): p. 153-156.
66. Mashima, T., et al., *Identification of actin as a substrate of ICE and an ICE-like protease and involvement of an ICE-like protease but not ICE in VP-16-induced U937 apoptosis.* Biochemical and biophysical research communications, 1995. **217**(3): p. 1185-1192.
67. Mashima, T., et al., *Aspartate-based inhibitor of interleukin-1β-converting enzyme prevents antitumor agent-induced apoptosis in human myeloid leukemia U937 cells.* Biochemical and biophysical research communications, 1995. **209**(3): p. 907-915.
68. Enari, M., et al., *A caspase-activated DNase that degrades DNA during apoptosis, and its inhibitor ICAD.* Nature, 1998. **391**(6662): p. 43-50.
69. Yoshida, A., et al., *Opioid analgesic-induced apoptosis and caspase-independent cell death in human lung carcinoma A549 cells.* International journal of molecular medicine, 2000. **6**(3): p. 329-364.
70. Horvath, R.J. and J.A. DeLeo, *Morphine enhances microglial migration through modulation of P2X4 receptor signaling.* Journal of Neuroscience, 2009. **29**(4): p. 998-1005.
71. Dutta, R., et al., *Morphine modulation of toll-like receptors in microglial cells potentiates neuropathogenesis in a HIV-1 model of coinfection with pneumococcal pneumoniae.* Journal of Neuroscience, 2012. **32**(29): p. 9917-9930.
72. Merighi, S., et al., *Morphine mediates a proinflammatory phenotype via μ-opioid receptor–PKCε–Akt–ERK1/2 signaling pathway in activated microglial cells.* Biochemical pharmacology, 2013. **86**(4): p. 487-496.
73. Merighi, S., et al., *Cannabinoid CB2 receptor attenuates morphine-induced inflammatory responses in activated microglial cells.* British journal of pharmacology, 2012. **166**(8): p. 2371-2385.
74. Gessi, S., et al., *The activation of μ-opioid receptor potentiates LPS-induced NF-kB promoting an inflammatory phenotype in microglia.* FEBS letters, 2016. **590**(17): p. 2813-2826.
75. Maduna, T., et al., *Microglia express mu opioid receptor: insights from transcriptomics and fluorescent reporter mice.* Frontiers in psychiatry, 2019. **9**: p. 726.
76. Tumati, S., et al., *Tachykinin NK1 receptor antagonist co-administration attenuates opioid withdrawal-mediated spinal microglia and astrocyte activation.* European journal of pharmacology, 2012. **684**(1-3): p. 64-70.
77. Vacca, V., et al., *Botulinum toxin A increases analgesic effects of morphine, counters development of morphine tolerance and modulates glia activation and μ opioid receptor expression in neuropathic mice.* Brain, behavior, and immunity, 2013. **32**: p. 40-50.
78. Eidson, L.N. and A.Z. Murphy, *Blockade of Toll-like receptor 4 attenuates morphine tolerance and facilitates the pain relieving properties of morphine.* Journal of Neuroscience, 2013. **33**(40): p. 15952-15963.
79. Eidson, L.N. and A.Z. Murphy, *Persistent peripheral inflammation attenuates morphine-induced periaqueductal gray glial cell activation and analgesic tolerance in the male rat.* The Journal of Pain, 2013. **14**(4): p. 393-404.
80. Zöllner, C., et al., *Chronic morphine use does not induce peripheral tolerance in a rat model of inflammatory pain.* The Journal of clinical investigation, 2008. **118**(3): p. 1065-1073.
81. Lin, S.-L., et al., *Predicting neuroinflammation in morphine tolerance for tolerance therapy from immunostaining images of rat spinal cord.* PloS one, 2015. **10**(10): p. e0139806.

82. Zadina, J.E., et al., *Endomorphin analog analgesics with reduced abuse liability, respiratory depression, motor impairment, tolerance, and glial activation relative to morphine.* Neuropharmacology, 2016. **105**: p. 215-227.
83. Roeckel, L.-A., et al., *Opioid-induced hyperalgesia: cellular and molecular mechanisms.* Neuroscience, 2016. **338**: p. 160-182.
84. Verkhratsky, A. and A. Butt, *Glial physiology and pathophysiology*. 2013: John Wiley & Sons.
85. Eddleston, M. and L. Mucke, *Molecular profile of reactive astrocytes—implications for their role in neurologic disease.* Neuroscience, 1993. **54**(1): p. 15-36.
86. Eng, L.F. and R.S. Ghirnikar, *GFAP and astrogliosis.* Brain pathology, 1994. **4**(3): p. 229-237.
87. Hernandez, M.R., et al., *Differential gene expression in astrocytes from human normal and glaucomatous optic nerve head analyzed by cDNA microarray.* Glia, 2002. **38**(1): p. 45-64.
88. Pekny, M. and M. Nilsson, *Astrocyte activation and reactive gliosis.* Glia, 2005. **50**(4): p. 427-434.
89. Pekny, M. and M. Pekna, *Astrocyte reactivity and reactive astrogliosis: costs and benefits.* Physiological reviews, 2014. **94**(4): p. 1077-1098.
90. Balasingam, V., et al., *Reactive astrogliosis in the neonatal mouse brain and its modulation by cytokines.* Journal of Neuroscience, 1994. **14**(2): p. 846-856.
91. Hostenbach, S., et al., *Astrocyte loss and astrogliosis in neuroinflammatory disorders.* Neuroscience letters, 2014. **565**: p. 39-41.
92. Klein, M.A., et al., *Impaired neuroglial activation in interleukin-6 deficient mice.* Glia, 1997. **19**(3): p. 227-233.
93. Rabchevsky, A.G., et al., *A role for transforming growth factor α as an inducer of astrogliosis.* Journal of Neuroscience, 1998. **18**(24): p. 10541-10552.
94. Sriram, K., et al., *Induction of gp130-related cytokines and activation of JAK2/STAT3 pathway in astrocytes precedes up-regulation of glial fibrillary acidic protein in the 1-methyl-4-phenyl-1, 2, 3, 6-tetrahydropyridine model of neurodegeneration: key signaling pathway for astrogliosis in vivo?* Journal of biological chemistry, 2004. **279**(19): p. 19936-19947.
95. Winter, C.G., et al., *A role for ciliary neurotrophic factor as an inducer of reactive gliosis, the glial response to central nervous system injury.* Proceedings of the National Academy of Sciences, 1995. **92**(13): p. 5865-5869.
96. Pekny, M. and M. Pekna, *Reactive gliosis in the pathogenesis of CNS diseases.* Biochimica et Biophysica Acta (BBA)-Molecular Basis of Disease, 2016. **1862**(3): p. 483-491.
97. Machelska, H. and M.Ö. Celik, *Opioid receptors in immune and glial cells—implications for pain control.* Frontiers in immunology, 2020. **11**: p. 300.
98. Tu, H., et al., *The role of the M1/M2 microglia in the process from cancer pain to morphine tolerance.* Tissue and Cell, 2020: p. 101438.
99. Zhang, Q., et al., *DAMPs and autophagy: cellular adaptation to injury and unscheduled cell death.* Autophagy, 2013. **9**(4): p. 451-458.
100. Farina, C., F. Aloisi, and E. Meinl, *Astrocytes are active players in cerebral innate immunity.* Trends in immunology, 2007. **28**(3): p. 138-145.
101. Farina, C., et al., *Preferential expression and function of Toll-like receptor 3 in human astrocytes.* Journal of neuroimmunology, 2005. **159**(1-2): p. 12-19.
102. Bsibsi, M., et al., *Broad expression of Toll-like receptors in the human central nervous system.* Journal of Neuropathology & Experimental Neurology, 2002. **61**(11): p. 1013-1021.
103. Park, C., et al., *TLR3-mediated signal induces proinflammatory cytokine and chemokine gene expression in astrocytes: differential signaling mechanisms of TLR3-induced IP-10 and IL-8 gene expression.* Glia, 2006. **53**(3): p. 248-256.
104. Gorina, R., et al., *Astrocytes are very sensitive to develop innate immune responses to lipid-carried short interfering RNA.* Glia, 2009. **57**(1): p. 93-107.

105. Jack, C.S., et al., *TLR signaling tailors innate immune responses in human microglia and astrocytes.* The Journal of Immunology, 2005. **175**(7): p. 4320-4330.
106. Campbell, I.L., et al., *Neurologic disease induced in transgenic mice by cerebral overexpression of interleukin 6.* Proceedings of the National Academy of Sciences, 1993. **90**(21): p. 10061-10065.
107. Chiang, C.-S., et al., *Reactive gliosis as a consequence of interleukin-6 expression in the brain: studies in transgenic mice.* Developmental neuroscience, 1994. **16**(3-4): p. 212-221.
108. Rossi, D., *Astrocyte physiopathology: at the crossroads of intercellular networking, inflammation and cell death.* Progress in neurobiology, 2015. **130**: p. 86-120.
109. Aschner, M., *Astrocytes as mediators of immune and inflammatory responses in the CNS.* Neurotoxicology, 1998. **19**(2): p. 269-281.
110. Minagar, A., et al., *The role of macrophage/microglia and astrocytes in the pathogenesis of three neurologic disorders: HIV-associated dementia, Alzheimer disease, and multiple sclerosis.* Journal of the neurological sciences, 2002. **202**(1-2): p. 13-23.
111. Suk, K., et al., *Activation-induced cell death of rat astrocytes.* Brain research, 2001. **900**(2): p. 342-347.
112. Bowie, A. and L.A. O'Neill, *The interleukin-1 receptor/Toll-like receptor superfamily: signal generators for pro-inflammatory interleukins and microbial products.* Journal of leukocyte biology, 2000. **67**(4): p. 508-514.
113. Dong, C., R.J. Davis, and R.A. Flavell, *MAP kinases in the immune response.* Annual review of immunology, 2002. **20**(1): p. 55-72.
114. Johnson, G.L. and R. Lapadat, *Mitogen-activated protein kinase pathways mediated by ERK, JNK, and p38 protein kinases.* Science, 2002. **298**(5600): p. 1911-1912.
115. Vallés, S.L., et al., *Chronic ethanol treatment enhances inflammatory mediators and cell death in the brain and in astrocytes.* Brain pathology, 2004. **14**(4): p. 365-371.

Preprints (www.preprints.org) | NOT PEER-REVIEWED | Posted: 10 March 2022 doi:10.20944/preprints202203.0153.v1

Figure legends

Fig. 1 Motor coordination and locomotion assessment in different groups using a rotarod and open field tests. (a) Methadone decreased motor coordination. Motor coordination was significantly impaired in the methadone-treated group in comparison with the control group at the 1st and 2nd weeks. (b) In methadone-treated group, the total distance traveled, which is a measure of spontaneous exploration in the open field area and a good indicator for motor ability in rats, decreased significantly compared to control group. (c) Presence at the center of the field, as an indicator of anxiety, decreased in the methadone group compared to the control group. (*P< 0.05; **P<0.01, ***P<0.001) (n=7). The values are expressed as means ± SEM.

Fig. 2 Methadone increased EMG latency. (a) The sciatic nerve stimulated and the muscle action potential recorded in the gastrocnemius muscle are shown as excitatory postsynaptic potential (EPSP). (b) The EMG latency increased significantly in the methadone-treated rats (**P< 0.01) (n = 7) compared to the control group. The values are expressed as means ± SEM.

Fig. 3 Immunohistochemistry against caspase-3 was performed in various groups. The analysis showed that the administration of methadone increased the expression of caspase-3 positive cells. (*P<0.05; **P<0.01, ***P<0.001). The values are expressed as mean ± SEM (n = 3).

Fig. 4 Microgliosis in methadone-treated rats. (a) Immunohistochemistry against Iba-1 was performed for the methadone and the control groups, with the b Iba-1 exhibiting a surge in the methadone group. (c) Nearest neighbor distance (NND) was longer in the methadone group than in the control group (**P<0.01; ***P<0.001). The values are expressed as means ± SEM (n = 3)

Fig. 5 Quantitative microglia analyses. The results of Sholl analysis (n=30) showed that the complexity of microglia processes declined in the methadone group. (a) According to the microglia soma size measurement, the cell body significantly increased in the methadone-treated group. (b) The assessment of total microglia processes length showed the decreased length of this processes in the methadone group (c).). (*P<0.05; **P<0.01, ***P<0.001). The values are expressed as mean ± SEM.

Fig. 6 Immunohistochemistry against GFAP. The analysis showed the increased number of GFAP positive cells in the methadone group compared to the control (a,b). (*P<0.05; **P<0.01, ***P<0.001). The values are expressed as mean ± SEM, (n = 3). Nearest neighbor distance (NDD) (n=10) was significantly lower in the methadone group than in the control group (c).

Fig. 7 Quantitative astrocyte analyses (n=30). Complexity of astrocyte processes increased in methadone group compared to the control group (a). The measurement of astrocyte soma size showed a significant increase in the cell body in the methadone group (b). The assessment of total astrocyte processes length suggested that length of this processes increased in methadone group (c). The values are expressed as mean ± SEM. *P<0.05, **P<0.01, ***P<0.001.

 doi:10.20944/preprints202203.0153.v1

Fig. 8 Methadone induced several genes related to apoptosis, necroptosis and inflammation pathways. Real-time qPCR data showed that the expression level of inflammatory cytokines including TNF, was significantly increased under methadone treatment. Furthermore, methadone induced substantial increases in mRNA expression of apoptotic markers caspase-3. Moreover, necroptosis associated markers (RIPK3) showed a significant rise. Relative mRNA expression was normalized to GAPDH. The values are expressed as means (± SEM; n=3)

Preprints (www.preprints.org) | NOT PEER-REVIEWED | Posted: 10 March 2022 doi:10.20944/preprints202203.0153.v1

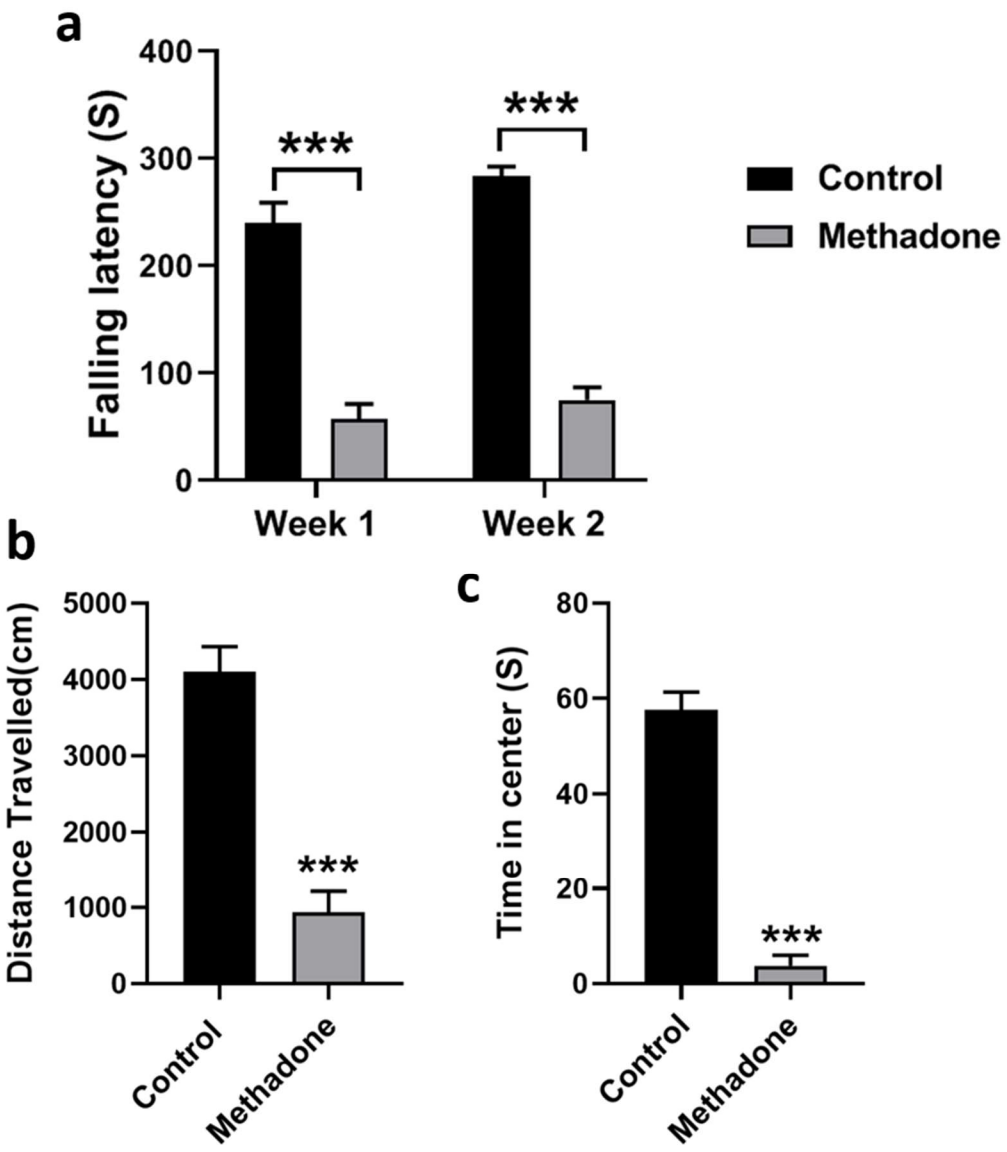

Fig.1

Preprints (www.preprints.org) | NOT PEER-REVIEWED | Posted: 10 March 2022 doi:10.20944/preprints202203.0153.v1

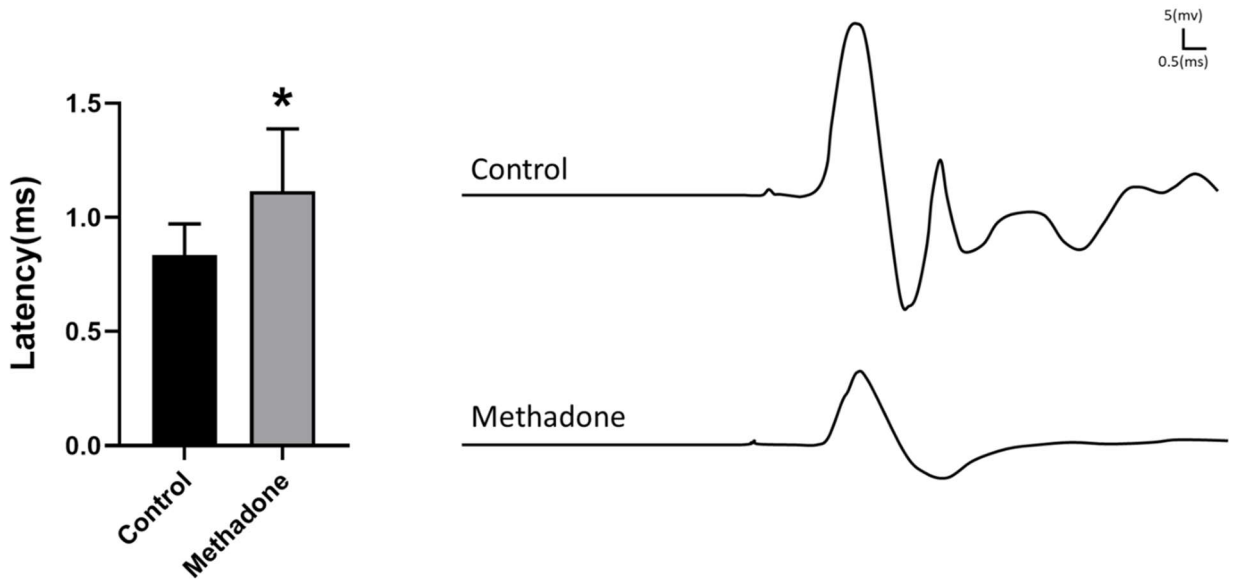

Fig.2

Preprints (www.preprints.org) | NOT PEER-REVIEWED | Posted: 10 March 2022 doi:10.20944/preprints202203.0153.v1

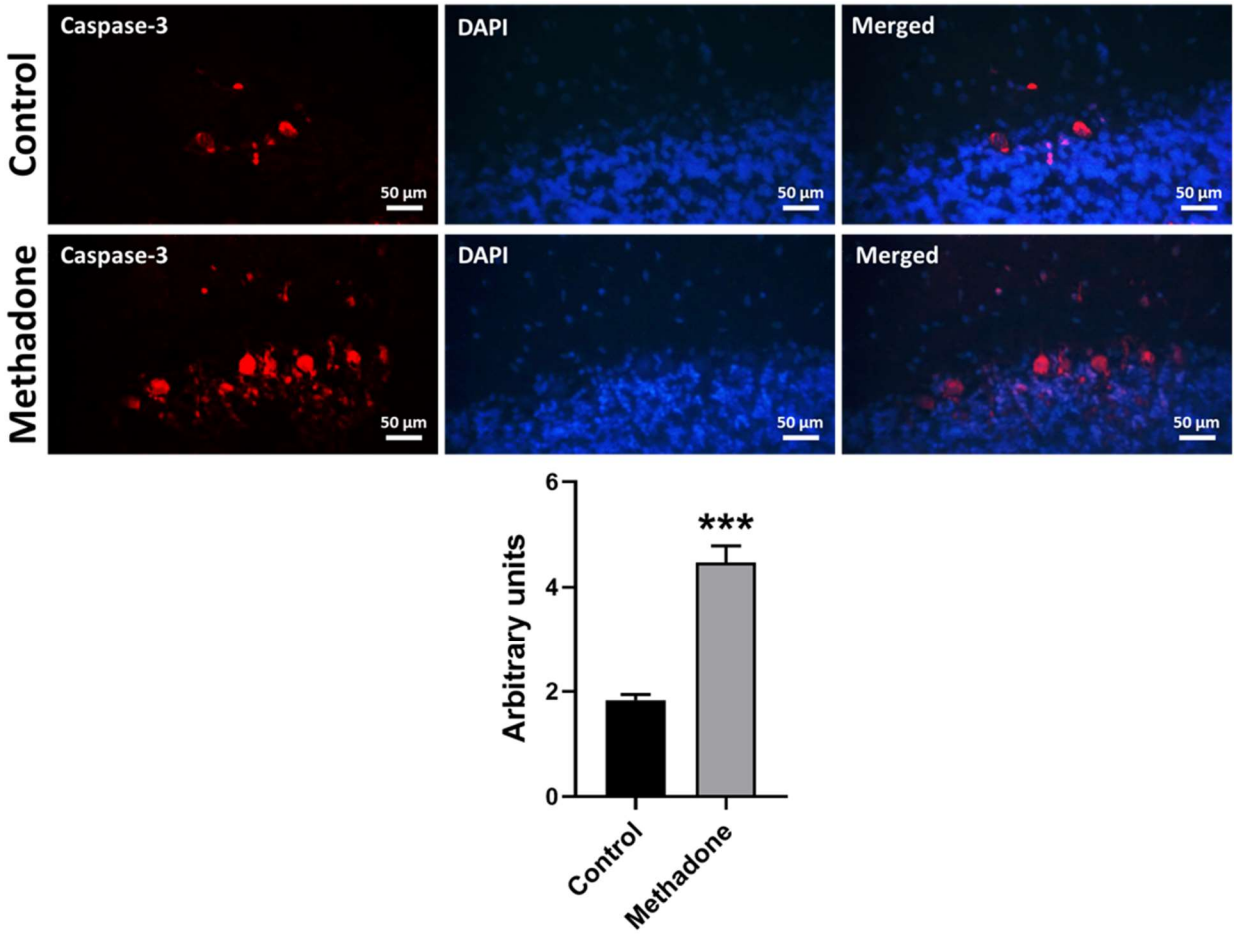

Fig.3

Preprints (www.preprints.org) | NOT PEER-REVIEWED | Posted: 10 March 2022 doi:10.20944/preprints202203.0153.v1

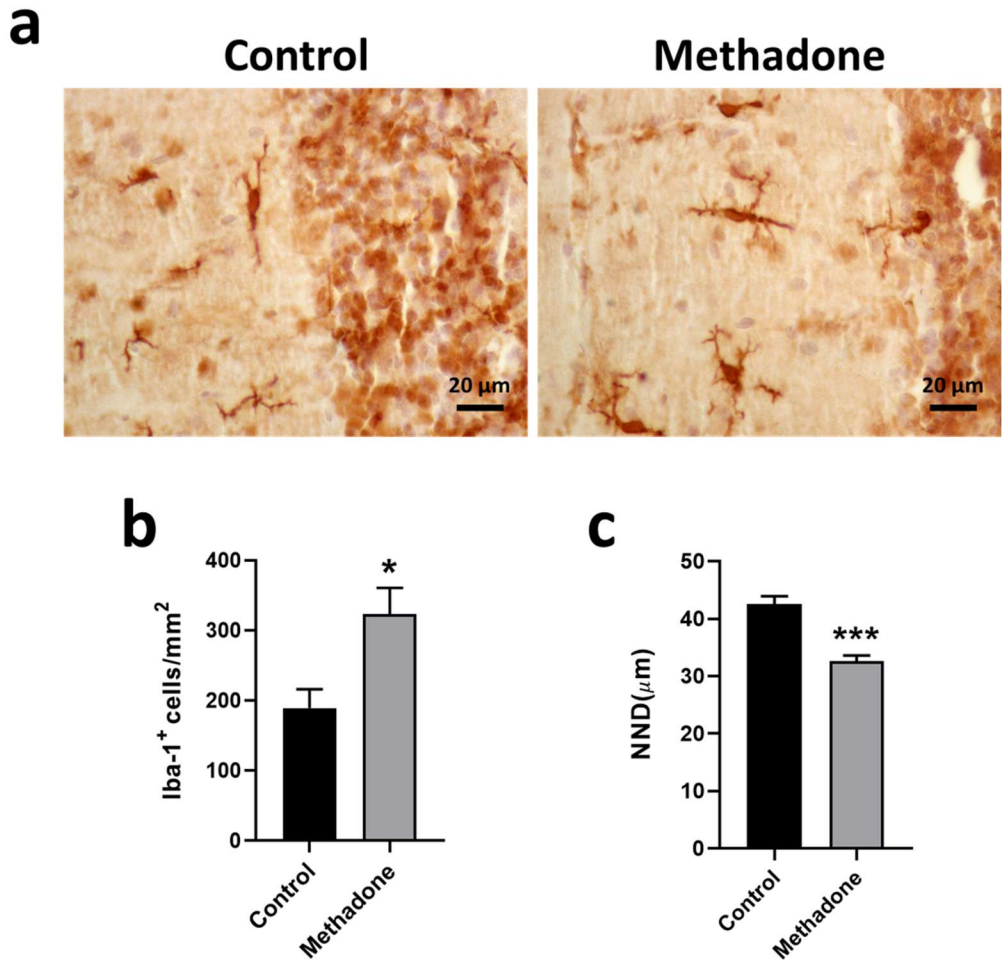

Fig.4

Preprints (www.preprints.org) | NOT PEER-REVIEWED | Posted: 10 March 2022 doi:10.20944/preprints202203.0153.v1

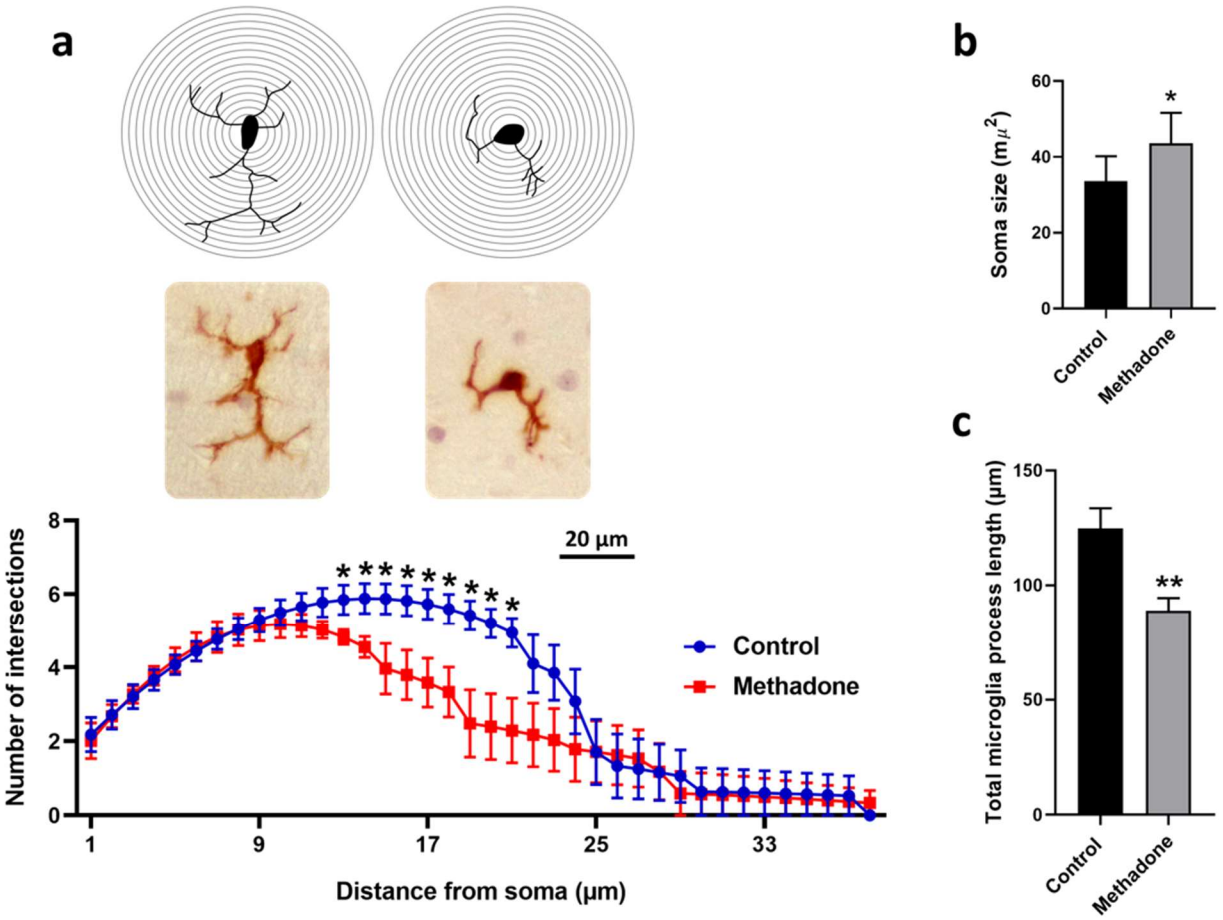

Fig.5

Preprints (www.preprints.org) | NOT PEER-REVIEWED | Posted: 10 March 2022 doi:10.20944/preprints202203.0153.v1

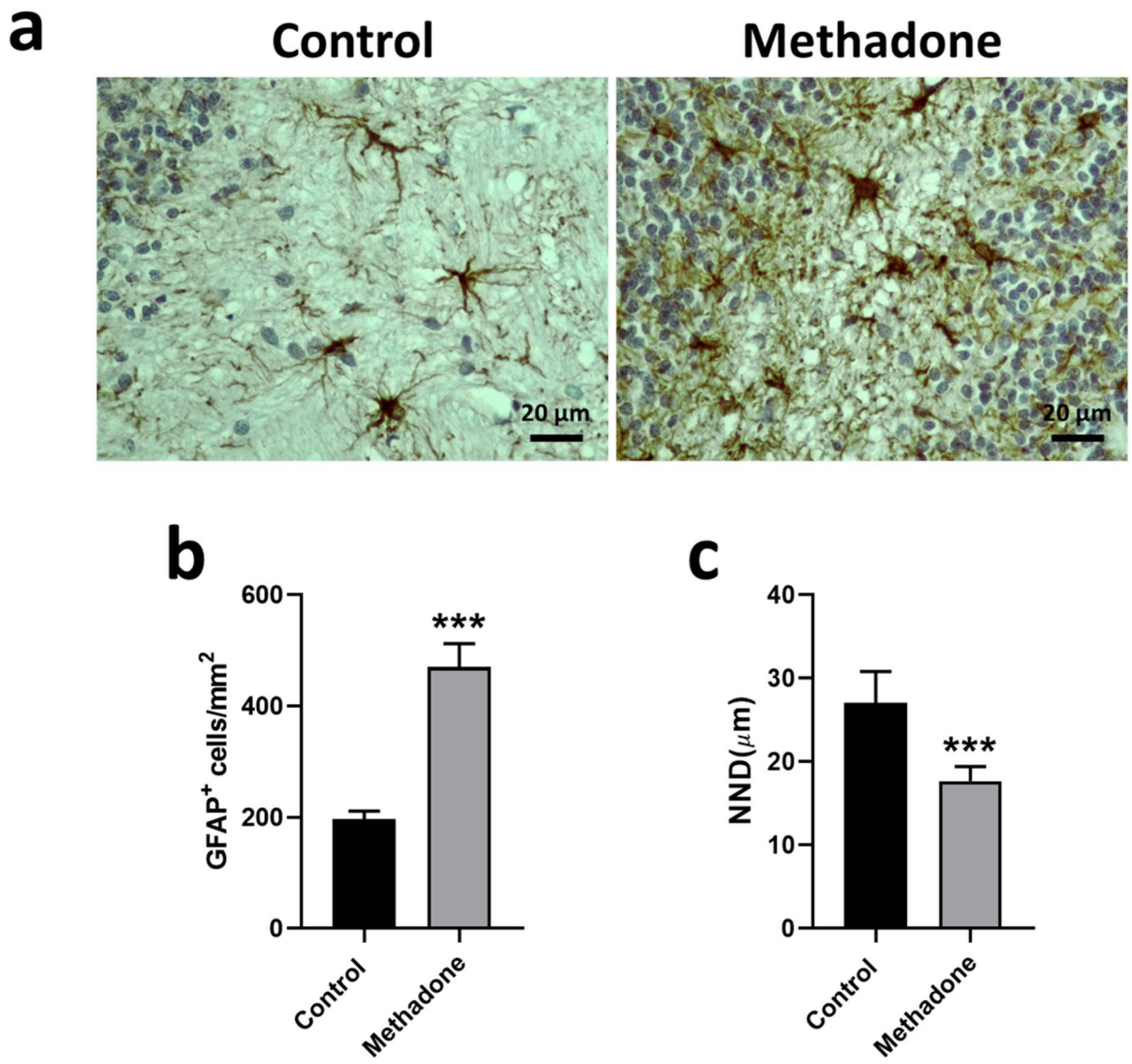

Fig.6

Preprints (www.preprints.org) | NOT PEER-REVIEWED | Posted: 10 March 2022 doi:10.20944/preprints202203.0153.v1

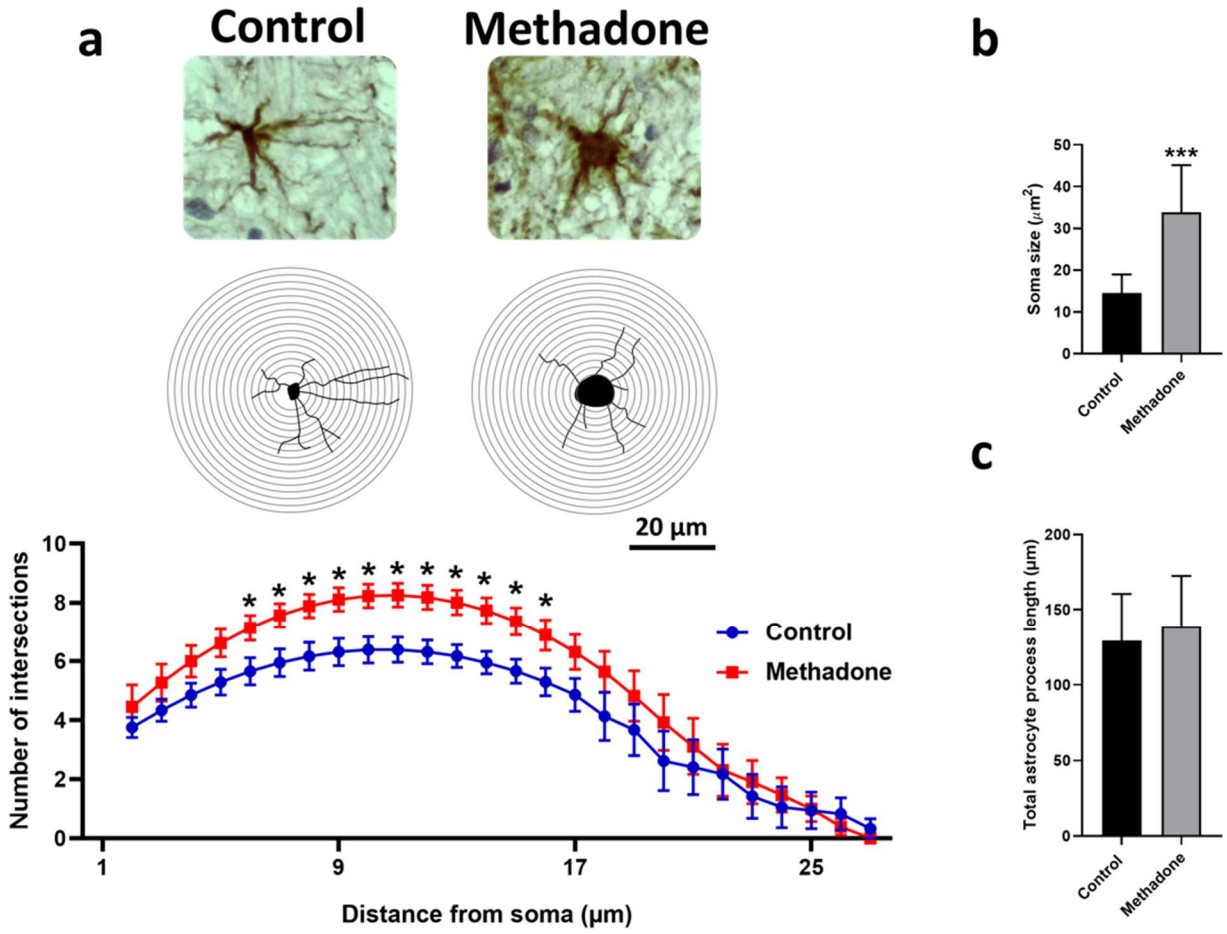

Fig.7

Preprints (www.preprints.org) | NOT PEER-REVIEWED | Posted: 10 March 2022 doi:10.20944/preprints202203.0153.v1

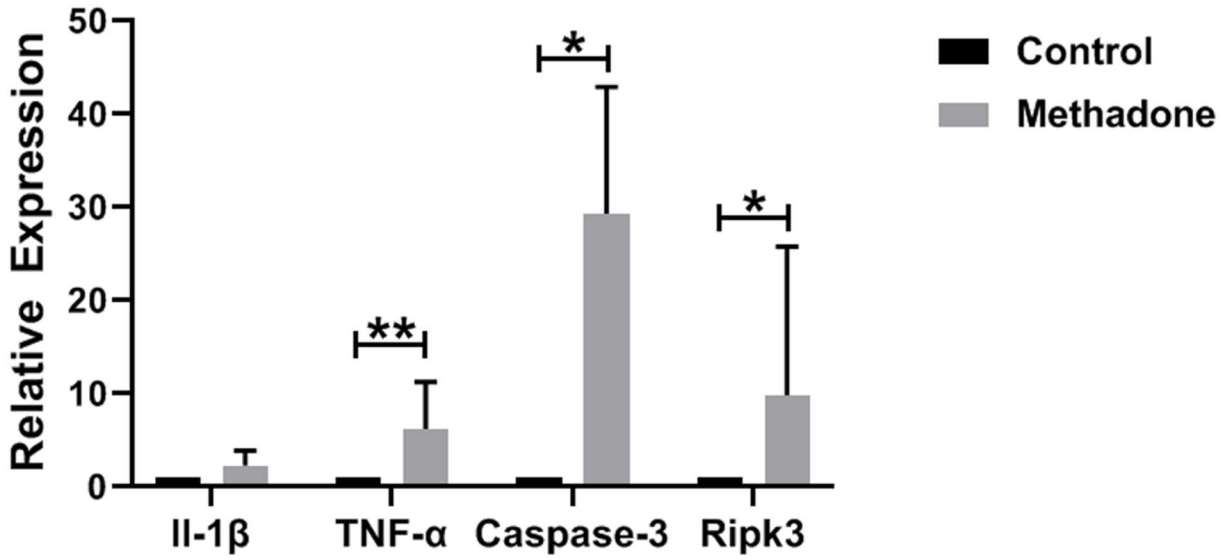

Fig.8

Preprints (www.preprints.org) | NOT PEER-REVIEWED | Posted: 10 March 2022 doi:10.20944/preprints202203.0153.v1

Table 1

Primer Name	Sequence	Annealing	Accession Number
Ripk3	F:5'GGAGTCAGGGGAATCAAGCC 3' R: 5'TTTGTAGTCTTTGACCTCTTGTTGG 3'	60°C × 25 s	NM_139342.2
IL1-ß	F:5'GGGAACTGTGCAGACTCAAACTC3' R: 5' AAAGAAGAAGATGGAAAAGCGGTT 3'	60°C × 25 s	NM_031512.2
TNF	F: 5' ACCACGCTCTTCTGTCTACTG 3' R: 5' CTTGGTGGTTTGCTACGAC 3'	60°C × 25 s	NM_012675.3
Caspase 3	F: 5' GGTATTGAGACAGACAGTGG 3' R: 5' CATGGGATCTGTTTCTTTGC 3'	55°C × 25 s	NM_012922.2
GAPDH	F: 5' ATGGAGAAGGCTGGGGCTCACCT 3' R: 5' AGCCCTTCCACGATGCCAAAGTTGT 3'	60°C × 25s	NM_017008.4